PAPER

A novel chip-based parallel transfection assay to evaluate paracrine cell interactions†

Elisabeth Kuhn,[a] Elisabeth Naschberger,[a] Andreas Konrad,[a] Roland S. Croner,[b] Nathalie Britzen-Laurent,[a] Ramona Jochmann,[a] Helmut Münstedt[c] and Michael Stürzl*[a]

The speed of gene function analyses in mammalian cells was significantly increased by the introduction of cell chip technology (reversely transfected cell microarray). However, the presently available technique is restricted to the analysis of autocrine effects of genes in the transfected cells. This limits the power of this method, as many genes are involved in heterotypic signaling both in physiologic and pathologic processes. At present, analyses of paracrine effects of transfected genes require trans-well or conditioned media approaches which are costly and time-consuming. Here, we present a novel method for the highly parallel analysis of paracrine gene functions on a chip. The basic idea was to adapt the cell chip technology to be performed with two different cell types which are differentially transfected: (1) an effector cell which is transfected with the genes of interest, and (2) an indicator cell in order to detect specific paracrine effects exerted from the transfected effector cells. Spot-to-spot diffusion of the paracrine mediators was prevented by matrix overlay, ultimately allowing 192 parallel tests for paracrine gene activations on one chip. In addition, we demonstrate the broad applicability and robustness of this technique using (1) various responder cell types, (2) various paracrine inducers, and (3) various indicator genes. The herein described approach allows for the first time a highly parallel analysis of paracrine gene functions and thus facilitates the characterization of genes involved in heterotypic cell communication in a broad range of research areas.

Introduction

High-throughput methods for gene expression analyses are constantly improving. Clusters of 50 to 100 genes that are differentially expressed within a specific disease or disease stage are often identified when these methods are applied to the molecular characterization of diseases.[1,2] In most cases, the pathogenic functions of these genes are unknown and further investigation is needed to understand these disease-related gene expression changes.

Ongoing research studies aim to increase the speed of gene function analyses in mammalian cells by automation of experimental processes and miniaturization of assays (for review see Stürzl *et al.*[3]). Recently, Ziauddin and Sabatini succeeded in scaling down high-throughput gene function analysis to the microarray level, allowing many parallel tests to be performed on a single chip.[4] In this method, different cDNA expression plasmids were printed onto slides together with a transfection reagent; the slides were placed in a culture dish and covered with adherent mammalian cells in the medium, and the final product, known as a reversely transfected cell microarray (RTCM, cell chip), consists of defined cell clusters that have been simultaneously transfected with different plasmids.[4] The RTCM procedure has been successfully used to investigate gene function in different cellular processes including signal transduction,[5] cell division,[6] apoptosis,[7] and secretion.[8] However, all of these approaches were limited to investigations of autocrine gene functions in the transfected cells.

Biological processes in multi-cellular organisms critically depend not only on autocrine but also on paracrine and juxtacrine gene effects. At present, common analyses of paracrine cell interactions include either trans-well approaches or harvesting of conditioned medium from one cell type to be subsequently applied to another physically separated cell type. Both methods are large-scale procedures that are costly and time-consuming.

Here, we describe a method for the highly parallel analysis of gene functions in paracrine cell interactions at the cell chip level. The basic idea was to adapt the technique of RTCM in order to be performed with two different cell types which are differentially transfectable: (1) effector cells which are transfected and

[a]*Division of Molecular and Experimental Surgery, Department of Surgery, University Medical Center Erlangen, Schwabachanlage 10, 91054 Erlangen, Germany. E-mail: michael.stuerzl@uk-erlangen.de; Fax: +49-9131-85-32077; Tel: +49-9131-85-33109*
[b]*Department of Surgery, University Medical Center Erlangen, Krankenhausstr. 12, 91054 Erlangen, Germany*
[c]*Institute of Polymer Materials, Friedrich Alexander University Erlangen-Nuremberg, Martensstr. 7, 91058 Erlangen, Germany*
† Electronic supplementary information (ESI) available. See DOI: 10.1039/c2lc20724a

subsequently secrete the paracrine mediator; and (2) indicator cells which are exposed to the paracrine mediator(s) released by the effector cells but are not transfected. Of note, this technology allows identification of genes involved in paracrine interactions *via* multiple ways. This includes that the gene introduced into the effector cells (1) may code directly for a secreted product which activates the indicator cells or (2) may induce or modify in the effector cell another factor which subsequently is secreted and activates the indicator cells. (3) Moreover, this method additionally allows screening of combination effects of paracrine active genes. In order to allow a highly parallel execution of different experiments on one chip, the diffusion of the different secreted paracrine mediators needs to be restricted to the vicinity of the respective transfection areas. Otherwise, assigning a paracrine gene effect to a specific transfection area is not possible.

Human embryonic kidney (HEK) cells are epithelial cells which can be efficiently transfected, exhibit high expression efficiencies, and are among the three cell lines most commonly used for protein production.[9–11] It has been shown that HEK cells are able to conduct most post-translational folding and processing steps necessary for protein function in mammalian cells.[10] HEK cells are small and can be grown to high cell density which supports the synthesis and secretion of high amounts of proteins. Due to these features, HEK 293T cells were chosen as effector cells for the following study. In contrast, indicator cells should be less efficiently transfected, a fact known from primary cells. We therefore used human primary fibroblasts (HFIBs) as indicator cells to establish the methodology. Of note, the paracrine crosstalk between epithelial cells and fibroblasts plays an important role in tumor invasion and inflammatory tissue reconstruction, which are major pathophysiologic processes in humans (for reviews see Mueller and Fusenig,[12] Coussens and Werb[13] and Liotta and Kohn[14]). Moreover, we demonstrated the broad applicability of the technique using different indicator cell types such as primary human umbilical vein endothelial cells (HUVECs), keratinocytes, and colorectal cancer cells which are of relevance for angiogenesis, wound healing, and cancer research, respectively.

Results and discussion

Selective reverse transfection of HEK 293T effector cells in combination with different indicator cell types

First, conditions had to be established that resulted in efficient reverse transfection of HEK 293T cells, but not of HFIBs (Fig. 1). To that goal, HEK 293T cells and HFIBs alone as well as a mixture of both cell types were subjected to reverse transfections with (1) increasing concentrations of a green fluorescent protein (GFP) expression plasmid, (2) four different transfection reagents [Effectene, Lipofectamine™ 2000 (both lipid-based), SuperFect (activated dendrimer) or calcium-phosphate (precipitates)], and (3) varying amounts of gelatin (Fig. 1a). Addition of gelatin to the transfection mix has been shown to increase the efficiency of reverse transfection.[4,5] GFP expression indicated that transfection in HEK 293T cells was most efficient using 0.75 µg to 1.5 µg of plasmid DNA together with Effectene or Lipofectamine™ 2000 (Fig. 1a), whereas no transfection

occurred with SuperFect or calcium-phosphate (data not shown). In addition, the transfection efficiency achieved with gelatin was higher than that achieved in the absence of gelatin for Lipofectamine™ 2000. No further increase was observed with gelatin concentrations from 0.05% up to 0.8% when using 0.75 µg and 1.0 µg DNA (Fig. 1a). Transfection efficiency achieved with 1.5 µg DNA and Lipofectamine™ 2000 was constant for gelatin concentrations from 0.2% up to 0.8% (Fig. 1a). Of note, the use of Effectene, but not of Lipofectamine™ 2000, resulted in scattered GFP-positive HEK 293T cells at a significant distance from the respective transfection areas (Fig. 1a, arrows). This may be due to increased migratory activity of transfected cells in the presence of Effectene. HFIBs alone did not show significant GFP expression with any of the different reverse transfection conditions tested (Fig. 1a, HFIB chip). On slides overlaid with mixtures of HEK 293T cells and HFIBs, speckled GFP signals were observed (Fig. 1a, HEK 293T/HFIB chip). In comparison to the homogeneous signals obtained in transfections with HEK 293T cells alone, this indicated the presence of a mixture of transfected and non-transfected cells, likely due to selective transfection of HEK 293T cells only. Based on these findings, all further experiments were performed using Lipofectamine™ 2000 with 1.5 µg DNA and 0.2% gelatin. These conditions resulted in high transfection efficiency, were in agreement with previous results[5] and caused the least scattering of transfected cells. Increased magnification of a transfection spot under these conditions showed that GFP was almost exclusively expressed in cells with cobblestone morphology (Fig. 1b, arrow), which is a hallmark of epithelial cells and indicates HEK 293T cells. In contrast, HFIB-like cells with spindle-shaped morphology were negative for GFP (Fig. 1b, arrowhead).

In order to further demonstrate the selective reverse transfection, the SV40 large T-antigen (T-antigen) was used as the specific marker, since it is selectively expressed in HEK 293T cells, but not in HFIB (ESI, Fig. S1a and c†). The RTCM was performed with an RFP expression plasmid using a mixture of HEK 293T cells and HFIB, followed by immunocytochemical detection of the T-antigen. Robust RFP expression was detected on every transfection spot, indicating successful reverse transfection (Fig. 1c). Detection of the T-antigen confirmed the selective transfection of HEK 293T cells (Fig. 1c, lower panel, arrow), and not HFIBs (Fig. 1c, lower panel, arrowhead).

In order to show that the assay can be applied to other cell combinations, HEK 293T cells were analyzed in combination with different other indicator cell types, such as keratinocytes (HaCaT), colorectal cancer cells (HT29 and WiDr), and primary human umbilical vein endothelial cells (HUVECs). These combinations were tested for selective transfection as previously described for HEK 293T/HFIB mixtures. Results clearly showed that in all cases only HEK 293T cells were transfected whereas none of the indicator cells were (Fig. 1d–g and S1b and d–g†).

In summary, the established conditions allow the selective reverse transfection of HEK 293T cells in combination with several different indicator cell types, thus providing a powerful tool for the analysis of paracrine cell interactions in a broad range of different applications. If not otherwise noted, a combination (1 : 3) of HEK 293T cells and HFIBs was used for all further experiments.
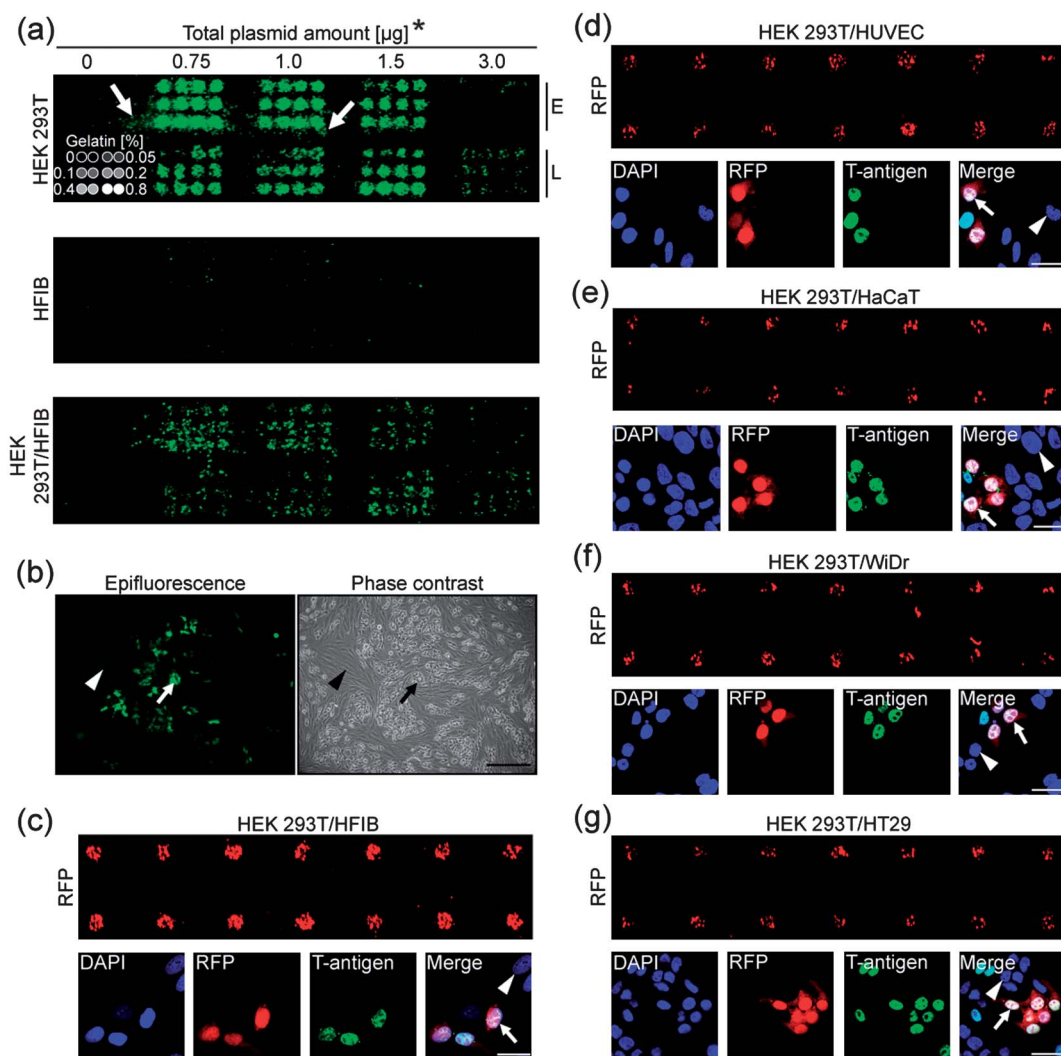
Fig. 1 Selective reverse transfection of HEK 293T cells in mixtures with various indicator cell types. (a) A GFP expression plasmid, transfection reagents [Effectene (E) and Lipofectamine™ 2000 (L)] and gelatin (concentrations in %, were used as shown in the inset spotting scheme) were printed in duplicates on glass slides. Subsequently, HEK 293T cells, HFIBs or a mixture of both cell types (1 : 3) were seeded, and GFP-expression was measured. Arrows indicate scattered GFP-expressing cells distant to the initial transfection area. *Total DNA amount added to the printing solution. (b) Epifluorescence (left) and phase contrast (right) pictures of a representative GFP transfection area on the HEK 293T/HFIB chip. Epithelial HEK 293T cells (arrows) and spindle-shaped HFIBs (arrowheads) are indicated. Scale bar = 250 μm (c–g) Selective reverse transfection of HEK 293T cells (arrow) with an RFP expression plasmid in mixture with various indicator cell types (arrowhead) such as: (c) HFIB (1 : 3), (d) HUVEC (1 : 3), (e) HaCaT (1 : 3), (f) WiDr (1 : 4), and (g) HT29 (1 : 4). An overview of the RFP transfection chip is shown (top), together with fluorescence images of representative transfection areas with DAPI staining, epifluorescence detection of RFP or immunofluorescence staining of SV40 large T-antigen (T-antigen). Scale bars = 25 μm.

Paracrine activation of indicator cells upon selective transfection of effector cells

In order to demonstrate paracrine activation of the indicator cells in a pretest, we used in the HEK 293T/HFIB setup interferon-γ (IFN-γ) as the inducer gene and guanylate binding protein-1 (GBP-1), a major IFN-γ-induced protein, as the indicator gene.[15,16] GBP-1 expression was highly induced by exogenously added recombinant IFN-γ in HFIBs, but not in HEK 293T cells (Fig. 2a), which allowed us to distinguish between HEK 293T cells and HFIBs. Moreover, supernatants harvested from HEK 293T cells classically transfected with an IFN-γ expression plasmid (pcDNA4-IFN-γ) contained high concentrations of IFN-γ (Fig. 2b) and induced GBP-1 expression in HFIBs, whereas supernatants from HEK 293T cells transfected with a control plasmid did not induce GBP-1 in HFIBs (Fig. 2c). These results showed that the IFN-γ encoded by pcDNA4-IFN-γ is efficiently expressed and secreted from HEK 293T cells and can paracrinely induce GBP-1 expression in HFIB. Reverse transfection with the IFN-γ expression plasmid or control plasmid on an HEK 293T/HFIB chip showed that (1) GBP-1 was only expressed in the presence of IFN-γ, and (2) GBP-1 was selectively expressed in HFIBs but not in the T-antigen-positive HEK 293T cells (Fig. 2d, merge). Furthermore, double staining of GBP-1 and IFN-γ confirmed that only HEK 293T cells (GBP-1-negative)
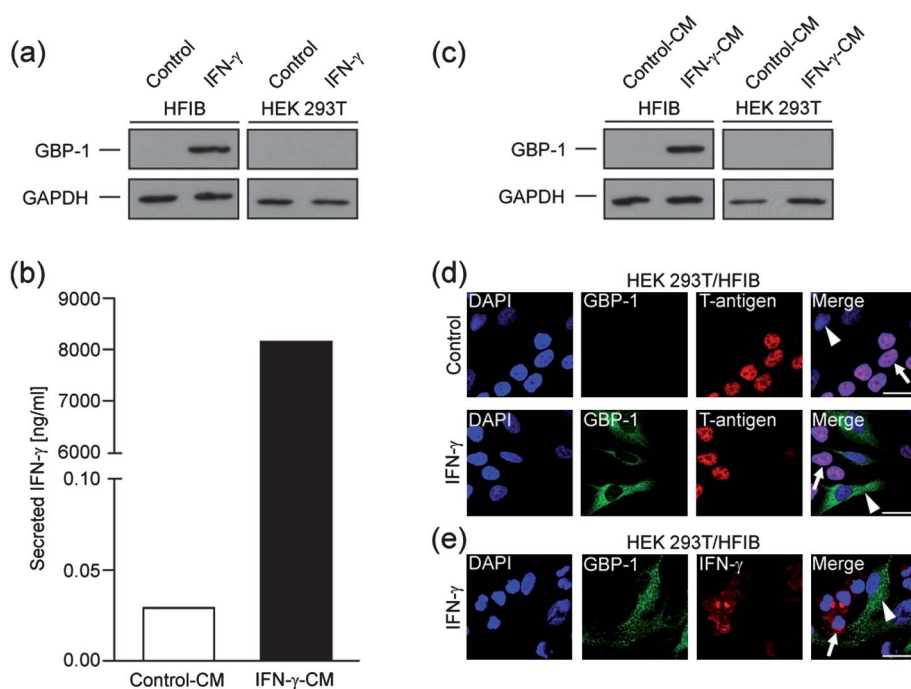
Fig. 2 Paracrine induction of GBP-1 expression by IFN-γ in HFIBs. (a) Western blot analysis of GBP-1 expression in HFIBs and HEK 293T cells that were either left unstimulated (control) or were stimulated for 24 h with 100 U ml^{-1} IFN-γ. Detection of GAPDH shows that equal amounts of protein were blotted onto the membrane. (b) Conditioned media of HEK 293T cells transfected with pcDNA4-IFN-γ (IFN-γ-CM) or control vector (control-CM) were harvested 48 h post-transfection, and the presence of secreted IFN-γ protein was determined by IFN-γ-ELISA. (c) Western blot analysis of GBP-1 expression in HFIBs and HEK 293T cells treated for 24 h with 20% IFN-γ-CM or control-CM. Detection of GAPDH shows that equal amounts of protein were blotted onto the membrane. (d and e) Selective reverse transfection of HEK 293T cells (arrow) with an IFN-γ expression plasmid (IFN-γ) or empty vector (control) in mixture with HFIB (arrowhead). Panels show DAPI staining and immunofluorescence staining of GBP-1, T-antigen, or IFN-γ. Scale bars = 25 μm.

expressed IFN-γ, whereas HFIBs (GBP-1-positive) did not (Fig. 2e, merge).

Restriction of diffusion by a matrix overlay

Diffusion of paracrine mediators from one transfection area to another can confound the analysis of highly parallel transfections that employ multiple different genes on a single chip. Therefore, gelatin, polyacrylamide (PAA), and Low-Melting Point (LMP) agarose were tested as matrices to be overlaid onto the chip to restrict diffusion. Each matrix was initially used in the highest concentration that allowed the formation of a homogeneous matrix. None of the matrices had cytotoxic effects in the used concentrations (data not shown). It was possible to completely remove the gelatin and LMP-agarose overlay after incubation for up to 48 h. In the case of PAA, a thin polyacrylamide layer remained on the slide, which may have disturbed subsequent immunocytochemical procedures for the detection of paracrine gene effects (see below). All three matrices were applied to HEK 293T/HFIB chips that had been printed with the IFN-γ expression plasmid. In the presence of a gelatin overlay or in conditions without a matrix overlay, GBP-1-expressing HFIBs were asymmetrically spread around the transfection spots without restriction (Fig. 3a). In contrast, PAA and LMP-agarose restricted diffusion as indicated by the reduced and more symmetric scattering of the GBP-1 expressing HFIBs around the transfection area (Fig. 3a). GBP-1 staining

was clearly stronger in the presence of LMP-agarose than in the presence of the PAA overlay (Fig. 3a). For quantitative comparison, the signal distributions were determined in two areas at the periphery of each transfection spot (Fig. 3b, upper panel). The mean values of the slopes of the respective linear regression curves (Fig. 3b, lower panel) were calculated and termed diffusion restriction index (DRI). An increasing DRI indicates an increasing capability of a matrix to restrict diffusion. This index was used to compare the different matrices. The DRI of LMP-agarose was significantly higher ($P < 0.001$) than the DRI values of the other matrices (Fig. 3c). Accordingly, LMP-agarose was used as matrix overlay for all further experiments.

In the next step, different concentrations of LMP-agarose were applied to a HEK 293T/HFIB chip with parallel transfections of pcDNA4-IFN-γ. At concentrations of up to 0.5% LMP-agarose, the DRI was significantly increased compared to the next lower concentration (Fig. 3d). A further but not significant decrease in diffusion was observed with 1% LMP-agarose (Fig. 3d). A LMP-agarose concentration of 2% resulted in a further decrease of signal spreading, but was also associated with lower signal intensity and increased spot heterogeneity (Fig. 3d, left). This decrease in signal spreading and intensity was due to cell loss during removal of the 2% LMP-agarose, which is no longer viscous at this concentration. Based on these findings, 1% LMP-agarose was used in all further experiments.

The diffusion of proteins of differing molecular weights is expected to vary. For this reason, IFN-γ was employed as the
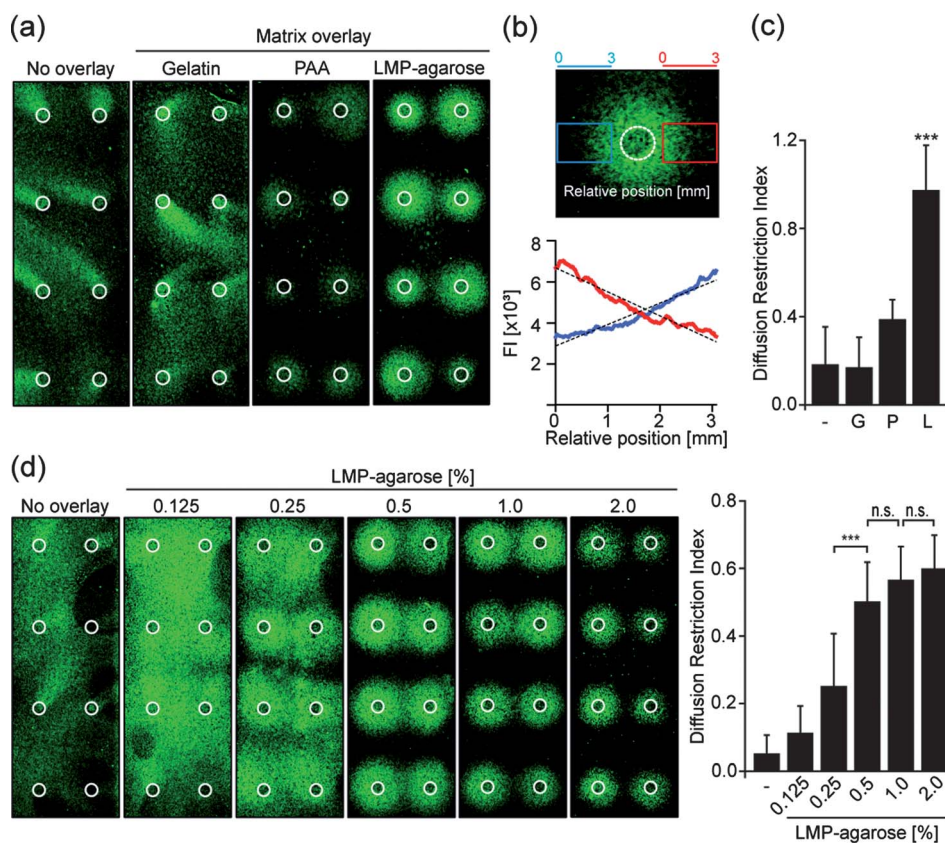
Fig. 3 Restriction of IFN-γ diffusion by matrix overlay after reverse transfection. (a) Immunofluorescence detection of paracrine-activated GBP-1 expression after reverse transfections on chips using an IFN-γ expression plasmid (1.0 μg per transfection mix), a mixture (1 : 3) of HEK 293T and HFIBs, and different matrix overlays [6% gelatin (G), 8000 ppm polyacrylamide (P), 1% LMP-agarose (L)]. Dashed white circles indicate application areas of the transfection mix. (b) Representative transfection spot with depicted areas (blue and red frames) used for signal quantification (upper panel). Graphs of fluorescence intensity (FI) distribution in the quantification areas (blue and red, lower panel) and corresponding linear regression curves (dashed black lines, lower panel). (c) The mean values of the slopes of the linear regression curves (see: b) of all eight transfections on each chip (see: a) were calculated and are shown as the diffusion restriction index (DRI) of each of the different matrices. The P-value is given in comparison to poly-acrylamide. ***, $P \leq 0.001$. (d) Reverse transfections analogous to (a) with increasing concentrations of LMP-agarose overlay in comparison to no matrix overlay (left). Bar diagram of the DRIs of the different overlays (right). n.s.: not significant; ***, $P \leq 0.001$.

effector gene for the optimization of the assay. IFN-γ has a molecular weight of 20 kDa. It thus represents a rather small protein with similar size to other physiologically and pathologically relevant paracrine acting factors such as TNF-α, IL-6, or IL-17.[17–20] Proteins of higher molecular weights are expected to diffuse less far through the matrix and will be even better restricted to the transfection area.

Highly parallel analysis of paracrine gene activities on one chip

Next, in order to further optimize the density of parallel transfection experiments on one chip, the minimal amount of plasmid required for paracrine-induced GBP-1 expression in HFIBs was determined. Decreasing amounts of pcDNA4-IFN-γ were printed on a HEK 293T/HFIB chip overlaid with 1% LMP-agarose. pcDNA4-IFN-γ in concentrations down to 8 ng per transfection mix still resulted in a clearly detectable GBP-1 signal in HFIBs (Fig. 4a). Using this concentration, 192 parallel transfection experiments for the analysis of paracrine gene functions could be performed on one chip and still allowed for a clear discrimination of each transfection area (Fig. 4b).

The comparison of pcDNA4-IFN-γ and empty vector transfected cell chips revealed a signal-to-background ratio of 164 and a signal-to-noise ratio of 13. This indicates that there is a clear increase between background compared to positive signals. The Z'-factor of the assay was calculated and is of 0.05, which corresponds to a "yes/no" type of answer (qualitative assay).[21] This demonstrates that the method can be applied to analyse whether single genes or combinations of genes induce in transfected effector cells paracrine activities on a specific feature of the indicator cells (for example adhesiveness for leukocytes, proliferation or specific signal transduction pathways).

Of note, the herein described method allows analyses of paracrine effects of transfected genes on a reduced cost basis caused by miniaturization of assay as compared to multi-well approaches. This is due to a significant reduction of the surface area per experiment (roughly 98% reduction compared to a 96-well and 90% reduction compared to a 384-well). Consequently, a considerably reduced amount of reagents is required, such as DNA or transfection reagent. In addition, the different experiments on a chip are subjected to identical experimental conditions and are not separated by different wells as compared
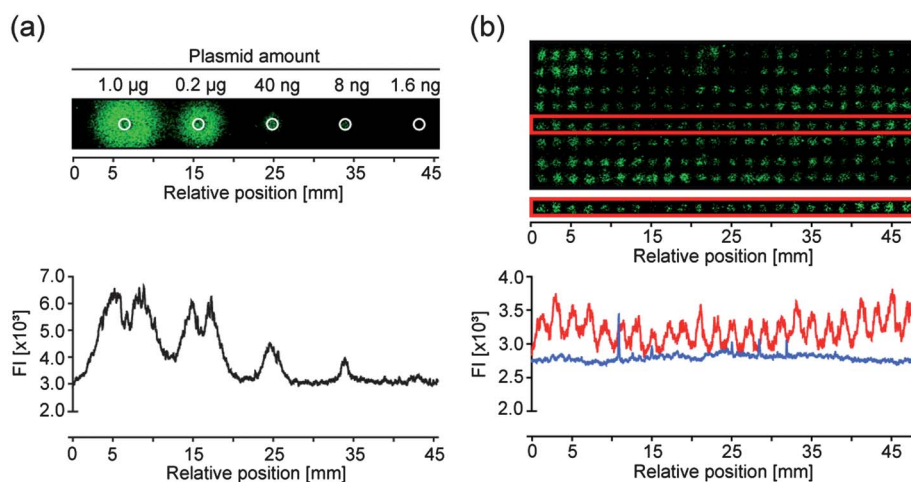
Fig. 4 Highly parallel analysis of paracrine gene activities on one chip. (a) Reverse transfections analogous to Fig. 3a with decreasing concentrations of the IFN-γ expression plasmid and an overlay with 1% LMP-agarose (upper panel). Diagram of the chip above showing the fluorescence intensities (lower panel). (b) High density reverse transfection chip with 192 analyses of paracrine IFN-γ-induced GBP-1 expression analogous to (a) with 8 ng IFN-γ expression plasmid per transfection mix (upper panel). Quantitative determination of the fluorescence intensities of the indicated transfection lane (upper panel, red frame) demonstrates spot to spot separation (lower panel, red line). The blue line represents the background signal obtained from a cell chip printed with an empty vector.

to multi-well approaches. Moreover, many replica slides can be produced out of one single spotting experiment, thus allowing to reproduce identical conditions for different applications and assay readouts.

Application of the new technique with different indicator cells, paracrine inducers, and different indicator genes

Finally, we investigated whether this method can be used with (1) different cell types, (2) different paracrine inducers, and (3) different indicator genes. We could show that TNF-α, but not IFN-α or IFN-γ transfection resulted in robust paracrine induction of COX-2 in the HEK 293T/HFIB setup, and of VCAM-1 and ICAM-1 in the HEK 293T/HUVEC setup (Fig. 5). All three indicator genes were paracrinely induced in the respective indicator cells (HFIB and HUVEC) as demonstrated by immunocytochemical double staining procedures showing that the indicator gene product was exclusively expressed in the indicator cells and not in the effector cells (Fig. 5, lower panels). These results demonstrated that the method is broadly applicable for many different screening approaches in a broad range of research areas such as inflammation and cancer.

Conclusion

In many different biological disciplines, the role of the microenvironment and paracrine intercellular communication is becoming increasingly appreciated. The method described here allows, for the first time, the analyses of gene functions in paracrine cell interactions at the biochip level. The major advantages of the established methodology are as follows: (1) the feasibility of highly parallel analyses, (2) the convenience of the handling procedure with the option to produce slides in advance for later applications, which may be of specific relevance for commercial purposes, (3) significantly reduced costs due to the miniaturization of the chip, which requires fewer cells, less DNA

and less transfection reagents, and (4) its robust performance which allows its broad applicability for many different cell types and indicator systems.

Over the past years, different gene clusters, typically consisting of 50 to 100 genes, have been identified by comparative transcriptome analyses to be associated with specific diseases or disease stages. However, in most cases it is still unclear how these genes contribute to the respective pathogenic process. The method described herein will be of specific advantage in the systematic investigation of single and combination effects of these disease-associated gene clusters in intercellular communication. In this framework many different applications of this method can be imagined. The specific examples shown here are screening approaches on (1) the induction of an IFN-γ-regulated Th1 immune reaction, which is associated with increased patient survival in colorectal cancer[22,23] (HEK 293T/HFIB setup, indicator gene: GBP-1), (2) the induction of tumorigenic pathways in stromal cells (HEK 293T/HFIB setup, indicator gene: COX-2), and (3) the inflammatory activation of endothelial cells (HEK 293T/HUVEC setup, indicator genes: ICAM-1 and VCAM-1). Of note, the screening approaches are not limited to immuno-fluorescence staining as readout. A wide range of readouts for the detection of morphologic transformation, proliferation, apoptosis, and cytotoxicity using respective staining procedures of indicator proteins or RNA are susceptible to this method. Moreover, paracrine activation of signaling programs in the indicator cells can be analyzed. To this goal, one can use indicator cells stably expressing a marker protein (e.g. GFP) under the control of a promoter which is activated by the signal transduction pathway of interest (for example NF-κB or p53). Furthermore, the method can be also used to determine interaction with a third cell type, such as immune cells adhering to endothelial cells which have been paracrinely stimulated by the effector cells. In this setup the matrix would be removed after the incubation time and immune cells would be added to the slides. Attachment of immune cells to indicator cells on or near a certain
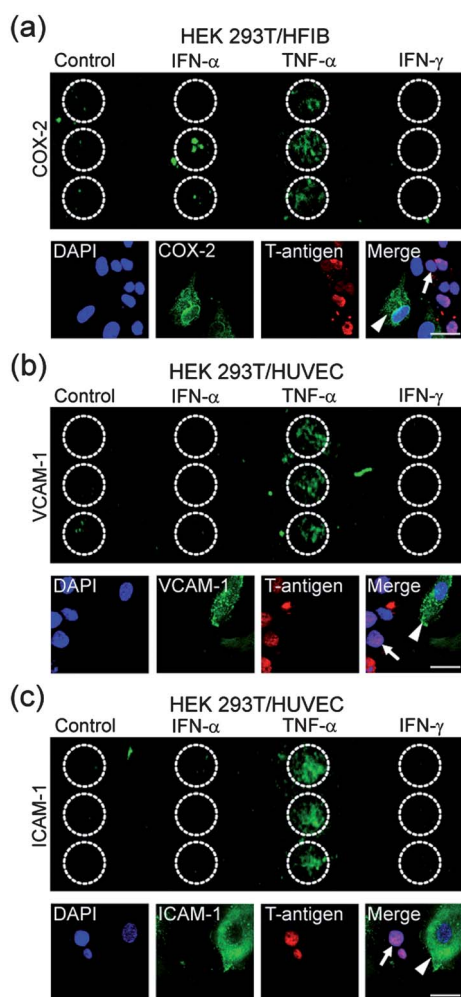
Fig. 5 Detection of paracrinely induced COX-2, VCAM-1, and ICAM-1 expression on HEK 293T/HFIB- and HEK 293T/HUVEC-chips. (a–c) Upper panels: overviews of selective reverse transfections of (a) HEK 293T/HFIB cell combinations (1 : 3), or (b and c) HEK 293T/HUVEC (1 : 3) cell combinations with IFN-γ-, TNF-α-, IFN-α-expression plasmids [(a) 0.2 μg per transfection mix, (b and c) 0.04 μg per transfection mix] or empty vector (control) (all in triplicates) and immunofluorescence staining of (a) COX-2, (b) VCAM-1 and (c) ICAM-1 expression. Lower panels: DAPI staining and immunofluorescence staining of T-antigen (arrow) and (a) COX-2, (b) VCAM-1 and (c) ICAM-1 (arrowheads) of representative TNF-α transfection areas. Scale bars = 25 μm. Dashed white circles indicate application areas of the transfection mixes.

transfection spot might then indicate paracrine activity of this specific effector gene. Finally, it is important to note that in the described setup, effector and indicator cells are in direct contact, which also allows for the analysis of juxtacrine gene effects. The described method illustrates a worthwhile approach for a convenient, low-cost and highly parallel analysis of paracrine cell communication.

Experimental

Cell culture

HEK 293T cells (CRL-11268™, ATCC, Manassas, VA, USA), human keratinocytes (HaCaT, DKFZ, Heidelberg, Germany), human colorectal cancer cells (WiDr, CCL-218™, ATCC), and primary human fibroblasts (HFIBs, PromoCell, Heidelberg, Germany) were cultivated in DMEM-10% FCS [Dulbecco's modified Eagle's medium (PAA Laboratories, Cölbe, Germany) supplemented with 10% fetal calf serum (FCS; Biochrom, Berlin, Germany), 2 mM L-glutamine, 100 U ml^{-1} penicillin and 100 μg ml^{-1} streptomycin (all three from PAA Laboratories)] at 37 °C in a humidified atmosphere with 8.5% CO$_2$. Primary human umbilical vein endothelial cells (HUVECs, Cambrex Bio Science, Verviers, Belgium) were cultivated in EGM-2-MV [endothelial cell culture medium (Lonza, Cologne, Germany) supplemented with 1× Antibiotic–Antimycotic Solution (100 U ml^{-1} penicillin, 100 μg ml^{-1} streptomycin, 250 μg ml^{-1} amphotericin B; all three from PAA Laboratories)] at 37 °C in a humidified atmosphere with 5% CO$_2$. The human colorectal cancer cell line HT29 (HTB-38™, ATCC) was cultivated in McCoy's 5A supplemented with 10% fetal calf serum (Biochrom), 2 mM L-glutamine (PAA Laboratories) at 37 °C in a humidified atmosphere with 5% CO$_2$.

All cells except HUVEC were maintained in uncoated tissue culture flasks. HUVEC were cultivated in flasks coated for at least 2 h with 1.5% bovine skin gelatin, type B (Sigma-Aldrich, Seelze, Germany) in PBS.

For propagation, 90% confluent cells were washed with 1× phosphate buffered saline (PBS) (Biochrom AG, Berlin, Germany), detached with 1 × 0.5 g l^{-1} trypsin and 0.2 g l^{-1} ethylene-diamine-tetra-acetic acid in HBSS (trypsin/EDTA) (PAA Laboratories) and reseeded on a fourfold increased area (one passage). HFIBs were used between passages 5 and 15 and HUVECs between passages 8 and 11. All cells were monthly tested for mycoplasma contamination using the MycoAlert Mycoplasma Detection Kit (Lonza) and were in all cases negative.

For stimulation with IFN-γ, HEK 293T cells and HFIBs were incubated overnight in DMEM-0.5% FCS and subsequently treated for 24 h with 100 U ml^{-1} recombinant human IFN-γ (Roche, Mannheim, Germany) in the same medium. IFN-γ was diluted in PBS containing 0.1% bovine serum albumin (BSA) (Sigma-Aldrich). As a control, the same volume of PBS/0.1% BSA was used, without IFN-γ.

Plasmids

An expression plasmid for human IFN-γ was constructed by amplifying a 501 bp long cDNA fragment corresponding to the full-length IFN-γ coding sequence (GenBank accession number NM_000619) from mRNA isolated from phorbol 12-myristate 13-acetate (200 ng ml^{-1}, Sigma-Aldrich) stimulated (18 h) Jurkat cells. The forward primer harbored a restriction site for BamHI (underlined) and a Kozak sequence (italics) (5′-CGC GGATCC*GCCACC*ATGAAATATACAAGTTATATCTTGG CTTTTCAG-3′), and the reverse primer contained a restriction site for EcoRV (underlined) (5′-TGCGATATCTTACTGG GATGCTCTTCGACCTC-3′). The PCR product was subjected to restriction digest with BamHI and EcoRV and inserted into the BamHI and EcoRV sites in pcDNA4-Myc/His (Invitrogen, Karlsruhe, Germany). The final construct (pcDNA4-IFN-γ) was confirmed by full-length sequencing of the inserted gene. Expression plasmids for human TNF-α and human IFN-α were kindly provided by Zhao, X. J. (Gene Therapy Program and

Alcohol Research Center, Louisiana State University Health Sciences Center, New Orleans, LA, USA) and S. Indraccolo, respectively (Istituto Oncologico Veneto, Istituto di Ricovero e Cura a Carattere Scientifico, Padua, Italy). Plasmids encoding green fluorescent protein (GFP; pEGFP-C1) or red fluorescent protein (RFP; pDsRed1-N1) were purchased from Clontech (BD Biosciences, Heidelberg, Germany).

Preparation of conditioned medium

HEK 293T cells were seeded in 1.5 ml at a density of 3×10^5 cells per well in a six-well plate 24 h prior to transfection. Cells were transiently transfected with 3 μg pcDNA4-IFN-γ or empty vector (pcDNA4) using the calcium-phosphate precipitation technique. Seven hours after transfection, the cells were washed twice with $1\times$ PBS, and 1 ml fresh DMEM-0.5% FCS was added to each well. The conditioned medium (CM) was harvested 48 h post-transfection, subjected to centrifugation ($4000 \times g$, 5 min, 4 °C) and directly used for further experiments.

Human IFN-γ enzyme-linked immunosorbent assay (ELISA)

IFN-γ protein expression in cell culture supernatants was determined with a Quantikine hIFN-γ-ELISA according to the manufacturer's instructions (R&D Systems, Abingdon, United Kingdom).

Western blot analysis

Cell extracts (10 μg) were separated by electrophoresis on 10% SDS-PAGE gels and analyzed by western blot as described previously.[24] The following primary antibodies were used: monoclonal rat anti-human GBP-1 antibody (1 : 500; clone 1B1[25]) and monoclonal mouse anti-human GAPDH antibody (1 : 70 000; Chemicon/Millipore, Schwalbach, Germany). Rabbit anti-rat and rabbit anti-mouse immunoglobulin G antibody coupled to horseradish peroxidase (both from Dako, Hamburg, Germany) were used as secondary antibodies at a 1 : 5000 dilution. Protein detection was performed using the enhanced chemiluminescence western blot detection system (ECL, GE Healthcare, Munich, Germany) and Rx-films (Fuji, Tokyo, Japan).

Diffusion restricting matrices

All matrix solutions were prepared fresh before use as follows: (1) bovine skin gelatin, type B (Sigma-Aldrich) was added to double-distilled water (56 °C). The solution was stirred for 20 min at 56 °C, cooled down to 37 °C and sterilized by filtration (0.45 μm). Subsequently, an identical volume of $2\times$ DMEM-10% FCS was added. (2) UltraPure low melting point agarose (LMP-agarose, Invitrogen) was dissolved in double-distilled water by heating in a microwave until the agarose was completely dissolved. Afterwards, the solution was adjusted to 37 °C, and an identical volume of $2\times$ DMEM-10% FCS was added. In case HUVECs were applied to the chip, the LMP-agarose was mixed with an identical volume of EGM-2-MV supplemented with 10% FCS and $2\times$ Antibiotic–Antimycotic Solution. (3) Neutral polyacrylamide (Sedipur NF 106, BASF SE, Ludwigshafen, Germany) was dissolved in DMEM-10% FCS and gently rotated until completely dissolved.

Prior to use, all matrices were pre-warmed to 37 °C and then gently added onto the slides with a serological pipette.

Selective reverse transfection

Plasmid DNA (0 μg to 3 μg per transfection mix) and gelatin (0% to 0.8%) were used as specified in the manuscript and the figures. In addition, four different transfection procedures were tested as described below:

(1) **Lipofectamine™ 2000 (Invitrogen).** The procedure using Lipofectamine 2000 was carried out according to the protocols described previously.[5,26] Briefly, DNA was resuspended in 5 μl double-distilled water, and then 3 μl Opti-MEM (Invitrogen) containing 0.4 M sucrose (Merck, Darmstadt, Germany) was added. Subsequently, 3.5 μl Lipofectamine™ 2000 was added, and the mix was incubated for 20 min at room temperature. Finally, 7.25 μl gelatin solution (prepared as described in the section titled "Diffusion restricting matrices") was added, resulting in a final volume of 18.75 μl.

(2) **Effectene (Qiagen).** Effectene was used according to the protocol described by Ziauddin and Sabatini[4] with modifications. DNA was resuspended in 15 μl DNA-condensation buffer (Buffer EC, Qiagen) containing 0.4 M sucrose. Subsequently, 1.5 μl enhancer solution was added, and the mixture was incubated for 5 min at room temperature. Then, 5 μl Effectene transfection reagent was added followed by 10 min incubation. Finally, 21.5 μl gelatin was added, resulting in a final volume of 43 μl.

(3) **SuperFect (Qiagen).** SuperFect has not been used for reverse transfection before (for review see Stürzl et al.[3]). Following the procedure described in the SuperFect transfection kit (Qiagen), DNA was resuspended in 30 μl Opti-MEM containing 0.4 M sucrose. SuperFect transfection reagent (10 μl) was added and incubated for 10 min at room temperature. Afterwards, 25.2 μl gelatin was added, resulting in a final volume of 65.2 μl. In addition to the ratios of DNA to gelatin, which is described in the manuscript, the effect of different ratios of DNA to SuperFect (1.5 μg DNA to 4, 8, 12.5 μl SuperFect) was tested. No significant differences in reverse transfection were observed (data not shown).

(4) **Calcium-phosphate precipitation.** Calcium-phosphate has not been previously tested in the reverse transfection procedure. Following the protocol of classical calcium-phosphate precipitation,[27] DNA was resuspended in 20 μl of a 0.25 M calcium chloride solution containing 0.4 M sucrose. A total of 20 μl $2\times$ HEPES-buffered saline was added and the DNA was incubated for 10 min at room temperature. Afterwards, 25.2 μl gelatin was added, resulting in a final volume of 65.2 μl. The formation of homogeneous precipitates in the printed transfection solution was verified by phase contrast microscopy of the chip.

(5) **Chip production.** Chips were generated by using pre-cleaned Superfrost Plus slides (Thermo Scientific, Menzel GmbH, Braunschweig, Germany), a VersArray ChipWriter Pro (Bio-Rad, Munich, Germany) and PTS600 pins (600 μm

diameter; Anopoli, Eichgraben, Austria). For printing, 18.75 µl of each transfection mix was transferred into a 384-well plate (Nunc, Thermo Fisher Scientific, Roskilde, Denmark), which was used as a template plate. This template plate was kept at 12 °C, and the humidity was adjusted to 65% throughout the spotting procedure. The printed slides were dried for at least 12 h prior to use.

(6) Cell seeding, signal detection and restriction of diffusion. For cell seeding, 8-well FlexiPERM attachable silicone chambers (Greiner Bio One, Frickenhausen, Germany) were used. The inner separation walls of the silicone chambers were cut out with a sterile scalpel to generate a single chamber frame bordering a surface area of 10 cm². The resulting FlexiPERM incubation frame was cleaned with 70% ethanol and sterile double-distilled water, dried, and attached onto the printed slides. Subsequently, HEK 293T cells alone (1×10^6 cells per slide), HFIB alone (2.4×10^5 cells per slide) or a mixture of both (1.2×10^5 HEK 293T plus 2.4×10^5 HFIB per slide) were added. Further cell mixtures used here contained HEK 293T (1.2×10^5 cells per slide) together with HUVEC (2.4×10^5 cells per slide), HaCaT (2.4×10^5 cells per slide), HT29 (3.6×10^5 cells per slide), and WiDr (3.6×10^5 cells per slide), respectively. Mixtures of HEK 293T with HFIB, HaCaT, HT29, or WiDr were seeded in DMEM-10% FCS, whereas the mixture of HEK 293T and HUVEC was seeded in EGM-2-MV. The FlexiPERM incubation frame was removed after 48 h and the slides were gently washed by dipping them once into Tris-buffered saline ($1\times$ TBS) and dried. For detection of GFP, the cells were fixed with 4% buffered paraformaldehyde (10 min, Sigma-Aldrich) and mounted with fluorescence mounting medium (Dako, Hamburg, Germany). The slides were stored overnight at 4 °C and GFP signals were detected with a Fuji FLA-5000 laser scanner (Fujifilm, Düsseldorf, Germany) at a resolution of 25 µm scanning steps.

When diffusion restricting matrices were used, the medium was removed 5 h after the cells were seeded, and the respective pre-warmed matrix (37 °C) was gently poured onto the slides. The slides were further incubated for 43 h at 37 °C. Then, the matrix was removed, and the slides were washed gently (2 min) with $1\times$ TBS and subjected to immunofluorescence analysis.

Immunofluorescence analysis

Chips with reversely transfected cells were washed with $1\times$ TBS, dried at room temperature, and fixed with 4% buffered paraformaldehyde (10 min, Sigma-Aldrich) 48 h after cell seeding (in the case of immunofluorescence analysis of VCAM-1 expression, the staining was performed 72 h after cell seeding). The slides were treated with 0.1% saponin (Sigma-Aldrich) (in $1\times$ TBS, 30 min) and incubated with 10% goat normal serum (GNS; Dianova, Hamburg, Germany) for 10 min. As primary antibodies, a monoclonal mouse anti-SV40 large T-antigen antibody (1 µg ml⁻¹; PAb416, Calbiochem/Merck, Darmstadt, Germany), a monoclonal rat anti-human GBP-1 antibody (1 : 100; clone 1B1[25]), a monoclonal mouse anti-human cyclooxygenase-2 (COX-2; 0.25 µg ml⁻¹; CX229; Cayman Chemical, Ann Arbor, Michigan, USA), a monoclonal mouse anti-human vascular cell adhesion molecule 1 (VCAM-1; 10 µg ml⁻¹; 1.4C3; Sigma-Aldrich) or a monoclonal mouse anti-human

inter-cellular adhesion molecule 1 (ICAM-1; 2 µg ml⁻¹; BBIG-I1; R&D Systems) were added in 5% GNS for 2.5 h. The slides were incubated for 1 h with a goat anti-mouse Alexa488 antibody or a goat anti-rat Alexa488 antibody (1 : 500, Invitrogen). The nuclei were counterstained (10 min) with 4′,6-diamidino-2-phenylindole (DAPI) (1 µg ml⁻¹, Invitrogen) and the slides were mounted with fluorescence mounting medium (Dako). All incubations were carried out at room temperature in a humidity chamber. Mounted slides were stored overnight at 4 °C before analysis with a Fuji FLA-5000 laser scanner and/or a Leica TCS SP5 confocal microscope (Leica Microsystems, Wetzlar, Germany), equipped with the LAS-LAF software.

Double-immunofluorescence staining was performed as described above with the following alterations: primary antibodies were applied in mixtures [(1) monoclonal rat anti-human GBP-1 antibody (1 : 100; clone 1B1) and monoclonal mouse anti-SV40 large T-antigen antibody (1 µg ml⁻¹; PAb416), (2) monoclonal rat anti-human GBP-1 antibody (1 : 20; clone 1B1) and monoclonal mouse anti-human IFN-γ antibody (1 : 800; clone 25718), (3) monoclonal mouse anti-human COX-2 antibody (0.25 µg ml⁻¹; CX229) and polyclonal rabbit anti-SV40 large T-antigen antibody (1 : 200; v-300; Santa Cruz, Heidelberg, Germany), (4) monoclonal mouse anti-human VCAM-1 (10 µg ml⁻¹; 1.4C3) and polyclonal rabbit anti-SV40 large T-antigen antibody (1 : 200; v-300), or (5) monoclonal mouse anti-human ICAM-1 (2 µg ml⁻¹; BBIG-I1) and polyclonal rabbit anti-SV40 large T-antigen antibody (1 : 200; v-300)] for 2.5 h. Detection of primary antibodies was carried out for procedures 1 and 2 by adding a mixture of goat anti-rat Alexa488 and highly cross-absorbed goat anti-mouse Alexa546 antibody (both 1 : 500; Invitrogen) and for procedures 3, 4 and 5 by adding a mixture of goat anti-mouse Alexa488 and goat anti-rabbit Alexa546 antibody (both 1 : 500; Invitrogen) to the slide.

Analysis of fluorescence intensity

Fluorescence signal intensities were determined with a laser scanner (FLA-5000, Fujifilm) and analyzed using the Aida software package (version 4.15; Raytest, Straubenhardt, Germany). Scanning was performed with an increment of 25 µm. In Fig. 4a and b, the entire indicated area was evaluated.

Statistical analysis

Student's *t* tests for independent samples were performed using the SPSS 18.0 software for Microsoft Windows (SPSS Inc., Chicago, IL, USA).

The signal-to-noise ratio and the Z'-factor were calculated as follows using a chip as described in Fig. 4b: 8 ng of pcDNA4-IFN-γ per transfection mix (positive control; signal) or empty vector (negative control; background) were printed 192 times on one slide. The total fluorescence intensity (FI) of each region of paracrinely induced HFIBs was measured and normalized to the respective area. The local background was subtracted from this FI, and these values were used for the calculation of the mean values and standard deviations (SD) of the positive and negative control. The signal-to-background ratio (S/B), signal-to-noise ratio (S/N), and the Z'-factor were calculated as follows:[21]

$$S/B = \frac{\text{mean signal}}{\text{mean background}}$$

$$S/N = \frac{\text{mean signal } - \text{ mean background}}{\text{SD of background}}$$

Z'-factor $=$
$$1 - \frac{3\text{SD of positive control } + 3\text{SD of negative control}}{|\text{mean of positive control } - \text{ mean of negative control}|}$$

Acknowledgements

References

1 T. R. Golub, D. K. Slonim, P. Tamayo, C. Huard, M. Gaasenbeek, J. P. Mesirov, H. Coller, M. L. Loh, J. R. Downing, M. A. Caligiuri, C. D. Bloomfield and E. S. Lander, *Science*, 1999, **286**, 531–537.

2 L. J. van 't Veer, H. Dai, M. J. van de Vijver, Y. D. He, A. A. Hart, M. Mao, H. L. Peterse, K. van der Kooy, M. J. Marton, A. T. Witteveen, G. J. Schreiber, R. M. Kerkhoven, C. Roberts, P. S. Linsley, R. Bernards and S. H. Friend, *Nature*, 2002, **415**, 530–536.

3 M. Stürzl, A. Konrad, G. Sander, E. Wies, F. Neipel, E. Naschberger, S. Reipschläger, N. Gonin-Laurent, R. E. Horch, U. Kneser, W. Hohenberger, H. Erfle and M. Thurau, *Comb. Chem. High Throughput Screening*, 2008, **11**, 159–172.

4 J. Ziauddin and D. M. Sabatini, *Nature*, 2001, **411**, 107–110.

5 A. Konrad, E. Wies, M. Thurau, G. Marquardt, E. Naschberger, S. Hentschel, R. Jochmann, T. F. Schulz, H. Erfle, B. Brors, B. Lausen, F. Neipel and M. Stürzl, *J. Virol.*, 2009, **83**, 2563–2574.

6 B. Neumann, T. Walter, J. K. Heriche, J. Bulkescher, H. Erfle, C. Conrad, P. Rogers, I. Poser, M. Held, U. Liebel, C. Cetin, F. Sieckmann, G. Pau, R. Kabbe, A. Wunsche, V. Satagopam, M. H. Schmitz, C. Chapuis, D. W. Gerlich, R. Schneider, R. Eils, W. Huber, J. M. Peters, A. A. Hyman, R. Durbin, R. Pepperkok and J. Ellenberg, *Nature*, 2010, **464**, 721–727.

7 O. Mannherz, D. Mertens, M. Hahn and P. Lichter, *Genomics*, 2006, **87**, 665–672.

8 J. C. Simpson, C. Cetin, H. Erfle, B. Joggerst, U. Liebel, J. Ellenberg and R. Pepperkok, *J. Biotechnol.*, 2007, **129**, 352–365.

9 F. Wurm and A. Bernard, *Curr. Opin. Biotechnol.*, 1999, **10**, 156–159.

10 P. Thomas and T. G. Smart, *J. Pharmacol. Toxicol. Methods*, 2005, **51**, 187–200.

11 P. Karyala, N. D. Namsa and D. R. Chilakalapudi, *PLoS One*, 2010, **5**, e14408.

12 M. M. Mueller and N. E. Fusenig, *Nat. Rev. Cancer*, 2004, **4**, 839–849.

13 L. M. Coussens and Z. Werb, *Nature*, 2002, **420**, 860–867.

14 L. A. Liotta and E. C. Kohn, *Nature*, 2001, **411**, 375–379.

15 E. Guenzi, K. Töpolt, C. Lubeseder-Martellato, A. Jörg, E. Naschberger, R. Benelli, A. Albini and M. Stürzl, *EMBO J.*, 2003, **22**, 3772–3782.

16 E. Naschberger, T. Werner, A. B. Vicente, E. Guenzi, K. Töpolt, R. Leubert, C. Lubeseder-Martellato, P. J. Nelson and M. Stürzl, *Biochem. J.*, 2004, **379**, 409–420.

17 S. Mocellin, C. R. Rossi, P. Pilati and D. Nitti, *Cytokine Growth Factor Rev.*, 2005, **16**, 35–53.

18 J. L. Luo, S. Maeda, L. C. Hsu, H. Yagita and M. Karin, *Cancer Cell*, 2004, **6**, 297–305.

19 E. Tartour, A. Gey, X. Sastre-Garau, C. Pannetier, V. Mosseri, P. Kourilsky and W. H. Fridman, *Cancer Res.*, 1994, **54**, 6243–6248.

20 J. L. Langowski, X. Zhang, L. Wu, J. D. Mattson, T. Chen, K. Smith, B. Basham, T. McClanahan, R. A. Kastelein and M. Oft, *Nature*, 2006, **442**, 461–465.

21 J. H. Zhang, T. D. Chung and K. R. Oldenburg, *J. Biomol. Screening*, 1999, **4**, 67–73.

22 E. Naschberger, R. S. Croner, S. Merkel, A. Dimmler, P. Tripal, K. U. Amann, E. Kremmer, W. M. Brueckl, T. Papadopoulos, C. Hohenadl, W. Hohenberger and M. Stürzl, *Int. J. Cancer*, 2008, **123**, 2120–2129.

23 J. Galon, A. Costes, F. Sanchez-Cabo, A. Kirilovsky, B. Mlecnik, C. Lagorce-Pages, M. Tosolini, M. Camus, A. Berger, P. Wind, F. Zinzindohoue, P. Bruneval, P. H. Cugnenc, Z. Trajanoski, W. H. Fridman and F. Pages, *Science*, 2006, **313**, 1960–1964.

24 E. Naschberger, C. Lubeseder-Martellato, N. Meyer, R. Gessner, E. Kremmer, A. Gessner and M. Stürzl, *Am. J. Pathol.*, 2006, **169**, 1088–1099.

25 C. Lubeseder-Martellato, E. Guenzi, A. Jörg, K. Töpolt, E. Naschberger, E. Kremmer, C. Zietz, E. Tschachler, P. Hutzler, M. Schwemmle, K. Matzen, T. Grimm, B. Ensoli and M. Stürzl, *Am. J. Pathol.*, 2002, **161**, 1749–1759.

26 H. Erfle, B. Neumann, U. Liebel, P. Rogers, M. Held, T. Walter, J. Ellenberg and R. Pepperkok, *Nat. Protoc.*, 2007, **2**, 392–399.

27 F. L. Graham and A. J. van der Eb, *Virology*, 1973, **52**, 456–467.